Biomass Conversion and Biorefinery (2023) 13:11295–11309
https://doi.org/10.1007/s13399-022-03736-y

ORIGINAL ARTICLE

Evaluation of characteristic features of untreated and alkali-treated cellulosic plant fibers from *Mucuna atropurpurea* for polymer composite reinforcement

P. Senthamaraikannan[1] · S. S. Saravanakumar[1]

Received: 10 November 2022 / Revised: 27 December 2022 / Accepted: 28 December 2022 / Published online: 9 January 2023

Abstract
In this study, a newly identified *Mucuna atropurpurea* cellulosic fiber was alkalized, and the alkalization duration was optimized by chemical analysis. The conversion of hemicellulose from α-cellulose (58.74 ± 5.74 to 75.24 ± 5.26 wt.%) increased the fiber's crystalline fraction. The rise in the crystallinity index (24.01–49.89%) of the optimally alkalized MAF verified the augmentation in the crystalline fraction. Removal of peaks at 2357, 1730, and 1245 cm^{-1} in the Fourier-transform infrared spectroscopy of Optimally Alkalized MAF (OAMAF) demonstrated a drop in amorphous fraction. Progress in the maximum degradation peak (298–320 °C) was established by thermogravimetric analysis. Scanning electron microscopic (SEM) pictures exposed the occurrence of the contamination, wax, and lignin-free outer layer in the OAMAF. Removal of elements in the energy-dispersive X-ray (EDX) spectrum of OAMAF confirmed elimination of contaminations present on the exterior of the fiber. Tensile strength (274.6 ± 29.5 to 307.3 ± 24.12 MPa) and tensile modulus (2.88 ± 1.026 to 4.633 ± 0.94 GPa) of MAF were also enhanced after the optimal NaOH treatment.

Keywords *Mucuna atropurpurea* fiber · Alkalization · Cellulose · Chemical analysis · Tensile testing

1 Introduction

Increasing environmental consciousness motivates scientists to replace conventional nonbiodegradable materials using new biodegradable materials [1]. Manmade fiber–reinforced polymers are widely used nonbiodegradable materials in different domains, namely, construction, automobile, military, packaging, and electronics [2]. However, new guidelines and recommendations of environmental agencies have restricted the usage of manmade fiber–reinforced polymers. Cellulosic fiber-based fiber-reinforced plastics are partially biodegradable and have mechanical properties similar to synthetic fiber–reinforced composites [3]. So, consumption of plant-based cellulosic fibers is increasing daily, creating demand for plant fibers. Jute, coir, sisal, and banana are commonly used plant fibers in fabricating plant fiber–reinforced composites [4, 5]. However, the present demand for cellulosic fibers cannot be fulfilled by utilizing only conventional fibers. Searching for a new cellulosic fiber with suitable properties is the solution to meet the market demand. Fiber-yielding plants are abundantly available throughout the world. Studying the fundamental properties of fiber, namely, chemical composition, crystallographic information, mechanical properties, and thermal behaviors, is required. Cellulose, hemicellulose, lignin, and wax are common chemical constitutions present in fibers. Chemical composition of the fiber alters the fiber's characteristics [6]. The binding between cellulosic fibers and polymer resin largely relies on the surface topography of plant fibers. Generally, lignin, hemicellulose, wax, and pollutions occur at the exterior of the fiber, which weakens the binding ability with the matrix. Eliminating amorphous fractions and impurities from the fiber's surface may increase its binding ability with polymer resin [7]. Surface modifications are a proven method to remove the contaminants and amorphous fractions from the fiber surface [8]. Various researchers use sodium hydroxide treatment because of its low cost, simplicity, and effectiveness. Alkalization does not only eliminate the amorphous fraction in the fiber surface but also modify the chemical configuration of the fiber [9, 10]. These fluctuations in the chemical configuration may impact the fiber's crystalline, tensile, and thermal properties. Optimal alkalization

✉ S. S. Saravanakumar
sankarameena@yahoo.co.in

[1] Department of Mechanical Engineering, Kamaraj College of Engineering and Technology, Virudhunagar, Tamil Nadu, India

for the cellulosic fibers differs from one fiber to another fiber. So, the optimal alkalization of plant fibers needs to be studied [11]. Recently, Senthamaraikannan and Saravanakumar [12] extracted *Mucuna atropurpurea stem* fibers (MAF) and investigated their properties. They recommended performing surface treatment because of the existence of contamination on the external layer of the MAF. The impact of the alkalization depends on two important parameters: the alkali solution concentration and treatment timing. Recently, various researchers conducted the alkalization to the *Ventilago maderaspatana*, *Ziziphus nummularia*, *Grewia flavescens*, and *Ficus religiosa* root fiber by varying alkali treatment timing. By following this, in this article also alkali treatment was performed using 5% (w/v) NaOH solution, and alkalization duration varied from 15, 30, 45, 60, and 75 min. The influence of alkalization on various properties was examined.

2 Materials and methods

2.1 Materials

Matured *M. atropurpurea* stem, sodium hydroxide pellets, demineralized water, and hydrochloric acid were used in this study.

2.2 Extraction of raw MAF

Mucuna atropurpurea belongs to the climbing plants found in Asian countries. The matured stems of the *M. atropurpurea* plants were collected. For the retting procedure, the collected stems were submerged in water [13]. The fiber bundle was recovered after 7 days and rinsed with clean water. By warming the MAF for 1 day at 80 °C, the moisture was removed. The dried MAF was kept safely inside a zip cover to minimize biological infection and impurity deposition prior to composite fabrication [14].

2.3 Alkalization

Ten grams of NaOH pellets was dissolved in 200 ml demineralized water to prepare 5% (w/v) NaOH solution. Then, 5% (w/v) NaOH solution was prepared in five different beakers and dried MAFs (about 10 g) were submerged in the NaOH solution. The alkalization duration of the MAFs in the different beakers varied from 15, 30, 45, 60, to 75 min [15]. After the corresponding alkalization duration was completed, MAFs were removed from the NaOH solution. To avoid accumulation of extra sodium on the external layer of the fiber, the alkalized MAF were submerged for 5 min in a low-concentration HCl solution [16]. The HCl-treated MAF were placed in a drier at 70 °C for 2 days to eliminate the wetness. Alkalization process of *Mucuna atropurpurea* stem fiber is shown in Fig. 1.

2.4 Quantification of chemical composition

Using a process developed by Kurschner and Hoffer [17], we determined the cellulose fraction in the MAF. When determining the hemicellulose content of the fiber, neutral detergent fiber technique was used [18]. The APPITA P11s-78 protocol was followed to estimate the MAF lignin fraction [19]. The amount of wax in the fiber was measured according to a set of rules outlined by Conrad [20]. A moisture analyzer (Mettler Toledo, model HS153) determined the wetness in the MAF. The ash of the MAF was measured with the help of TAPPI protocols. Five replicas were taken for each analysis to obtain accurate outcomes [21].

2.5 Optimally NaOH-treated MAF

Table 1 shows the chemical analysis results for untreated and NaOH-treated MAF. The percentage of cellulose in the plant fibers is a determining factor of various properties, namely, mechanical, crystalline, and thermal properties. As a result, for usage as reinforcement in fiber-reinforced plastics, fibers with a larger cellulose content are preferred [22]. Compared with 60 min alkalized MAF, MAF alkalized for other timing

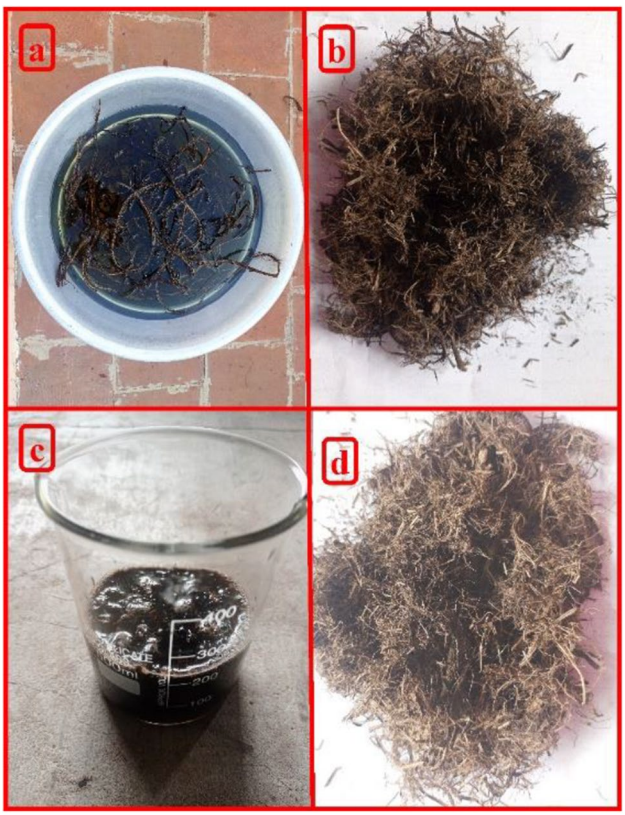

Fig. 1 **a–d** Alkalization process of *Mucuna atropurpurea* stem fiber

Table 1 Chemical compositions of raw and surface modified MAF

Alkalization duration	Density (kg/m^3)	Cellulose (wt.%)	Hemicelluloses (wt.%)	Lignin (wt.%)	Wax (wt.%)	Moisture content (%)	Ash (wt.%)
RMAF	1082 ± 29	58.74 ± 5.74	16.31 ± 3.21	14.22 ± 3.36	0.38 ± 0.08	11.12 ± 2.11	7.66 ± 2.49
15 min	1096 ± 22.14	64.14 ± 6.24	13.46 ± 4.21	12.11 ± 2.78	0.32 ± 0.12	10.62 ± 2.43	7.91 ± 2.66
30 min	1108 ± 24.31	68.74 ± 5.66	11.46 ± 3.37	10.46 ± 3.16	0.26 ± 0.09	8.22 ± 2.18	8.21 ± 2.77
45 min	1122 ± 19.34	72.33 ± 6.72	8.42 ± 2.88	8.22 ± 3.01	0.22 ± 0.08	7.64 ± 1.98	9.02 ± 2.33
60 minOAMAF	1136 ± 20.14	75.24 ± 5.26	7.96 ± 3.11	6.72 ± 2.88	0.18 ± 0.11	7.04 ± 1.78	9.88 ± 1.98
75 min	1149 ± 22.46	73.84 ± 4.48	6.88 ± 2.77	5.96 ± 2.69	0.15 ± 0.08	6.68 ± 1.81	10.21 ± 2.35

(15, 30, 45, and 75 min) and raw MAF (RMAF) have a lower cellulose percentage. So, MAF immersed in alkali solution for 60 min was considered as Alkalized fiber (OAMAF) [23].

2.6 Physical analysis

A liquid pycnometer was utilized to measure the density of RMAF and OAMAF. Toluene ($pt = 866$ kg/m^3) was used as the density-known fluid [24]. The diameter of the fibers was determined via a Model 7 Auslese optical microscope. The diameter of the 25 single fibers was calculated using ImageJ software and found to be same at four places in each fiber [25]. The average values of the four measurements for each fiber were noted for statistical examination.

2.7 Crystallographic investigation

X-Ray diffraction (XRD) examination was conducted using an X'Pert PRO-make diffractometer. In the sample container, a powdered fiber sample was placed, and an X-ray was passed through it. An X-ray sensor was employed to record the X-rays after diffraction. The rotation of the detector was restricted from $2\theta = 10$ to 80°, and it was moving $2\theta = 0.013°$ per 48.195 s. Using the following mathematical approach devised by Segal et al. [26], the crystallinity index (CI) of the RMAF and OAMAF was determined.

$$CI = \frac{I_C - I_A}{I_C} \times 100 \quad (1)$$

where I_C is the altitude of the diffractogram at 22° and I_A is the altitude of the diffractogram at 18°.

The fibers' crystallite size (CS) was measured via Eq. (2) [27]:

$$CS_{22} = \frac{0.89\ \lambda}{FWHM_{22} cos\left(\frac{2\theta}{2}\right)} \quad (2)$$

where λ is the wavelength of X-ray (1.54178 Å) and $FWHM_{22.42}$ is the full width at half maximum of the peak at 22°.

2.8 Determination of chemical functional groups

Fourier-transform infrared (FTIR) analysis of fiber was performed on a Jasco 6300 Type-A FTIR spectrometer [28]. Initially, powdered MAF and potassium bromide were finely blended at a ratio of 1:10. This blend was converted into a thin film by a hydraulic press. This film was exposed to infrared light at an incidence angle of 45°. Between the wavenumber of 4000 and 500 cm^{-1}, infrared light passing through the film was recorded at a scanning speed of 2 mm/s.

2.9 Nuclear resonance spectroscopy

NMR is a precious method to differentiate raw and surface modified fibers by determining chemical groups. A solid-state NMR (model ECX400; JEOL) was used to perform the nuclear magnetic resonance (NMR) analysis of RMAF and OAMAF. First, 300 mg fine powder was taken for analysis, and ^{13}C nuclei were chosen as the target. The experiment was run in the cross-polarization mode from 300 to − 100 ppm. The investigation was conducted at a resolution of 39.2824819 Hz and field strength was fixed as 399.7821 MHz [29].

2.10 Thermogravimetric analysis

The results of thermogravimetric analysis (TGA) may be utilized to determine the optimal processing temperature of a composite during fabrication and the optimal operating temperature of a composite made with the corresponding plant fiber [30]. TGA of the fibers were executed on an EXSTAR-6300 TGA machine. Initially, required quantities of fibers were taken into crucibles (alumina). Afterward, fiber-filled crucibles were placed in the heating chamber attached to the weighing machine. Temperature in the chamber was raised from 28 to 594 °C at a rate of 10 °C/min, while 200 ml/min of nitrogen gas was supplied constantly [31].

Calculation of kinetic activation (E_a) is an alternative way of understanding thermal behaviors of the fibers. In this investigation, E_a was determined using a simple graphical technique based on Eq. (3) established by Broido [32].

Table 2 Physical properties and chemical configurations of RMAF, OAMAF and other fibers

Name of the fiber	Untreated/alkalized	Physical properties		Chemical properties						References
		Diameter (μm)	Density (kg/m^3)	Cellulose (wt.%)	Hemicellulose (wt.%)	Lignin (wt.%)	Wax (wt.%)	Moisture content (wt.%)	Ash (wt.%)	
Kigelia africana fiber	Raw	–	–	55.1 ± 0.2	9.34 ± 0.08	11.7 ± 0.2	–	–	10.00 ± 0.4	[1]
	Alkalized	–	–	69.9 ± 0.1	9.01 ± 0.5	10.00 ± 0.4	–	–	1.3 ± 0.1	
Ziziphus nummularia fiber	Raw	209.064 ± 11	1322	52.34	18.64	13.43	0.63	10.45	12.34	[38]
	Alkalized	196.24 ± 10.2	1352	65.72	8.22	7.78	0.41	7.80	15.42	
Cocos nucifera L. var. typica fiber	Raw	0.323 ± 0.018	1360	50.11	11.98	24.90	0.31	11.10	1.60	[39]
	Alkalized	0.312 ± 0.012	1410	56.23	8.63	24.10	0.15	9.01	1.88	
Borassus fruit fiber	Raw	241.18	1256	68.94	14.03	5.37	0.64	6.83	–	[40]
	Alkalized	226.35	1265	82.85	3.02	5.02	0.49	8.04	–	
Saharan aloe vera cactus leaves fiber	Raw	91.15	1325.1	60.2	14.4	13.7	1.5	7.6	–	[9]
	Alkalized	80.61	1623.1	77.4	8.2	13.7	0.24	5.8	–	
Musa acuminata peduncles fiber	Raw	–	942	66.43	13.72	16.85	0.28	12.05	8.32	[41]
	Alkalized	–	992	74.22	8.58	7.91	0.17	6.72	11.32	
Ziziphus mauritiana fiber	Raw	570.2	1132	43	10.2	5.1	–	7.9	–	[42]
	Alkalized	368.5	1368	52	5.7	2.2	–	3.6	–	
Tridax procumbens fiber	Raw	233.1 ± 9.9	1160	32	6.8	3	0.71	11.2	–	[14]
	Alkalized	169.7 ± 9.2	1350	45	3.6	2.1	0.49	9.6	–	
Grewia flavescens fiber	Untreated	29.77 ± 2.805	1156	58.46	15.32	12.51	0.86	9.42	5.12	[22]
	Alkalized	25.35 ± 3.13	1176	68.31	11.54	7.85	0.53	6.55	8.81	
Symphirema involucratum fiber	Raw	168	1389	57.32	12.47	13.85	0.56	0.56	9.05	[15]
	Alkalized	153	1421	68.69	7.46	7.54	0.31	6.84	13.46	
Calotropis gigantea fruit bunch fiber	Raw	–	457	64.47	9.64	13.56	1.93	7.27	3.13	[16]
	Alkalized	–	469	69.93	6.72	11.25	1.12	6.12	4.86	
Bahunia racemosa fiber	Raw	–	–	68.9 ± 1.2	15.3 ± 0.6	14.2 ± 0.3	1.6 ± 0.5	10.1 ± 0.4	–	[43]
	Alkalized	–	–	74.9 ± 1.1	12.9 ± 0.6	11.3 ± 0.1	0.9 ± 0.6	10.8 ± 0.3	–	
Acacia concinna fiber	Raw	34.33 ± 6.42	1365	59.43	12.78	14.64	0.47	9.56	12.46	[23]
	Alkalized	32.76 ± 4.67	1384	68.56	8.56	8.38	0.33	7.67	14.32	
Ariel root of Ficus amplissima fiber	Raw	27.93 ± 0.917	1340	52.64	10.64	13.72	0.44	8.68	10.75	[44]
	Alkalized	23.87 ± 0.768	1357	61.67	6.22	8.15	4.82	0.16	14.46	
MAF	Raw	289 ± 21	1082 ± 29	58.74 ± 5.74	16.31 ± 3.21	14.22 ± 3.36	0.38 ± 0.08	11.12 ± 2.11	7.66 ± 2.49	[12]
	Alkalized	244.3 ± 14.38	1136 ± 20.14	75.24 ± 5.26	7.96 ± 3.11	6.72 ± 2.88	0.18 ± 0.11	7.04 ± 1.78	9.88 ± 1.98	This article

$$\ln\left[\ln\left(\frac{1}{y}\right)\right] = -\left(\frac{E_a}{8.32}\right)\left[\left(\frac{1}{T}\right) + K\right] \quad (3)$$

where T is the temperature of the fiber in Kelvin, y is the ratio of the mass of the fiber corresponding to the temperature (between 28 and 594 °C) and the mass of the MAF at 28 °C, and K is the reaction rate constant.

2.11 Surface morphological analysis

Surface modification of the plant fibers is mainly recommended to tailor the surface morphology to achieve improved binding between the plant fiber and matrix. Generally, during the alkalization, the external layer of the plant fibers is removed. This may improve the binding nature of the fiber [33]. On the other hand, alkalization for more than recommended timing may weaken the fiber's mechanical properties.

2.11.1 Scanning electron microscopic (SEM) analysis

SEM investigation of fibers was done in a 200 FEG SEM machine (FEI Quantum model). During the analysis, 50-Pa pressure was maintained around the worktable. To find the minute particle, impurities, and other materials around the surface fiber, images were captured at lower and higher magnifications (200×, 500×, 1000×, and 2000×). As plant fibers are nonconductive materials, a mild gold coating was applied on the fibers with the aid of sputter-coating equipment before being fixed onto the worktable. The accelerating voltage maintained for this investigation was 15 kV [34].

2.11.2 Energy-dispersive X-ray (EDX) analysis

This examination was conducted to find various elements existing around the fiber surface. It visualizes the difference between the surface of the surface modified and raw fiber. In this analysis, an EDX detector attached to the SEM machine recorded the different elements present on the RMAF and OAMAF. During the analysis, the current setting was modified to 25 pA [35].

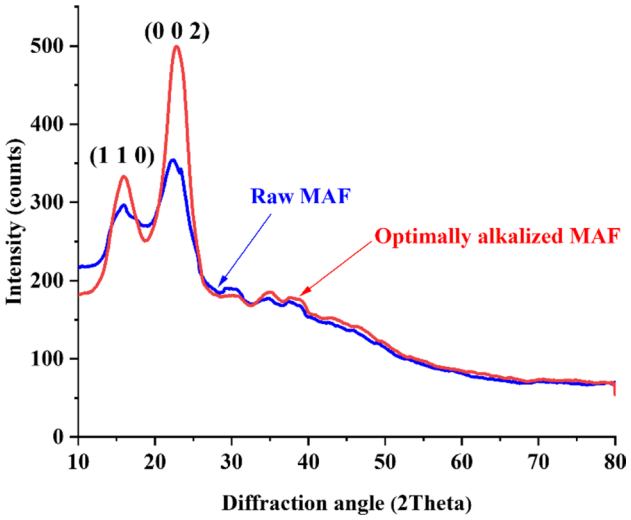

Fig. 3 X-Ray diffractograms of RMAF and OAMAF

2.11.3 Atomic force microscopic (AFM) analysis

AFM inspection provided 3D and 2D topographical pictures and surface morphological parameters, making it a more precise tool for evaluating the external surface of cellulosic fibers. By comparing surface morphological parameters of RMAF and OAMAF, the impact of surface modification can be easily understood. AFM analysis was conducted using an AFM machine (XE-70 type; Park) and operated in the non-conduct mode [13].

2.12 Tensile testing

In this study, the crosshead speed was operated with 2.5 mm per minute on a Zwick/Roell universal testing machine during single-fiber tensile testing. For testing, 25 fibers were chosen with the gauge length of 40 mm based on previous investigation [9, 12, 36]. The microfibril (α) angles of fibers were obtained via Eq. (4) [37].

$$\text{Strain rate} = \ln\left(1 + \frac{\text{Change in length}}{\text{Gauge length}}\right) = -\ln\ (\cos\ \alpha) \quad (4)$$

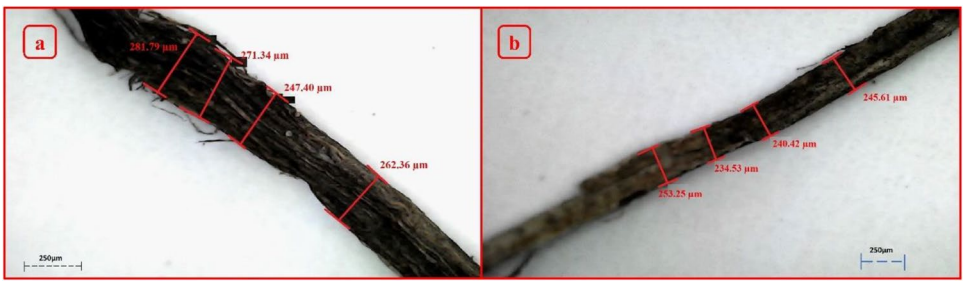

Fig. 2 Optical microscopy pictures of **a** RMAF and **b** OAMAF

3 Result and discussion

3.1 Quantification of chemical composition

Table 2 shows the weight percentage of chemical constitutions of RMAF and OAMAF, and various cellulose-based plant fibers. Owing to the conversion of amorphous fraction into α-cellulose, the cellulose fraction of OAMAF was increased noticeably (58.74 ± 5.74 to 75.24 ± 5.26 wt.%) [44]. This increased cellulose fraction was considered helpful in modification because it might considerably improve cellulosic fibers' mechanical and thermal stability [23].

Table 3 XRD, TGA, and tensile testing results of RMAF, OAMAF and other plant-based cellulosic fibers

Name of the fiber	Untreated/alkalized	Thermal properties		Crystalline properties		Tensile properties			Reference
		Thermal stability (°C)	Maximum degradation temperature (°C)	CI (%)	CS (nm)	Tensile strength (MPa)	Tensile modulus (GPa)	Strain rate (%)	
Kigelia africana fiber	Raw	–	–	59	–	379.28 ± 19.53	15.68 ± 2.92	2.61 ± 0.74	[1]
	Alkalized	–	–	60	–	411.08 ± 14.56	17.52 ± 1.72	3.68 ± 0.46	
Ventilago maderaspatana	Raw	200	335	25.88	26.12	383.7 ± 16.07	12.89 ± 0.811	4.59 ± 0.226	[11]
	Alkalized	200	349	28.21	23.34	408.4 ± 11.2	14.88 ± 0.974	4.11 ± 0.183	
Ziziphus nummularia fiber	Raw	225	348	45.77	2.05	247.3 ± 14.09	10.21 ± 1.29	1.54 ± 0.43	[38]
	Alkalized	233	360	50.6	3.52	307.9 ± 17.47	12.13 ± 1.56	1.24 ± 0.39	
Cocos nucifera L. var. typica fiber	Raw	250	–	52	6.5	154 ± 38	4.2 ± 0.7	3.6 ± 0.9	[39]
	Alkalized	250	–	60.84	9.8	201 ± 40	6.6 ± 1.1	2.9 ± 0.7	
Borassus fruit fiber	Raw	–	–	–	–	117.94	–	31.34	[40]
	Alkalized	–	–	–	–	175.52	–	32.72	
Saharan aloe vera cactus leaves fiber	Raw	–	350	52.6	5.6	621.8	40.03	2.47	[9]
	Alkalized	–	355	56.5	5.72	805.5	42.29	2.39	
Musa acuminata peduncles fiber	Raw	175	337	36.47	13.04	96.5 ± 32.7	2.22 ± 0.976	4.1 ± 1.7	[41]
	Alkalized	175	350	47.05	18.61	162 ± 53.7	3.46 ± 0.846	3.7 ± 1.4	
Ziziphus mauritiana fiber	Raw	280	360	31.70	43.5	32.7	–	–	[42]
	Alkalized	324	397	41.81	33.9	47.3	–	–	
Tridax procumbens fiber	Raw	195	250	34.46	25.04	25.75	0.94 ± 0.09	2.77 ± 0.27	[14]
	Alkalized	223	280	40.58	38.23	33.62	1.5 ± 0.270	2.30 ± 0.32	
Grewia flavescens fiber	Raw	165	325	16.01	62.90	276.9 ± 25.43	10.75 ± 1.303	3.384 ± 0.2243	[22]
	Alkalized	200	333	26.72	68.43	289.56 ± 28.56	13.78 ± 1.538	2.142 ± 0.4851	
Ficus religiosa root fiber	Raw	–	325	42.92	5.18	421.25 ± 18	5.11 ± 1.4	9.21 ± 2.3	[21]
	Alkalized	–	356	48.64	6.74	530.3 ± 23.70	8.02 ± 1.12	6.60 ± 0.53	
Symphirema involucratum fiber	Raw	200	350	28.22	5.10	471.2 ± 19.8	5.82 ± 0.77	6.77 ± 1.5	[15]
	Alkalized	200	371	33.33	3.21	397.22 ± 31	4.56 ± 1.3	5.84 ± 1.21	
Calotropis gigantea fruit bunch fiber	Raw	271	292	36	–	–	–	–	[16]
	Alkalized	282	317	39.8	–	–	–	–	
Bahunia racemosa fiber	Raw	–	313	79.4	–	–	–	–	[43]
	Alkalized	–	356	87	–	–	–	–	
Acacia concinna fiber	Raw	200	326	27.5	4.17	302.1 ± 16.78	8.544 ± 0.210	2.43 ± 0.265	[23]
	Alkalized	200	348	35.6	6.43	351.6 ± 16.12	10.39 ± 0.214	2.26 ± 0.182	
Ariel root of Ficus amplissima fiber	Raw	200	335	39	8.15	250.7 ± 11.26	7.76 ± 0.25	–	[44]
	Alkalized	230	347	43.33	11.28	278.4 ± 13.20	8.516 ± 0.358	–	
MAF	Raw	200	298	24.01	2.75	274.6 ± 29.5	2.88 ± 1.026	2.208 ± 0.654	[12]
	Alkalized	200	320	49.89	1.60	307.3 ± 24.12	4.633 ± 0.94	1.776 ± 0.56	Present article

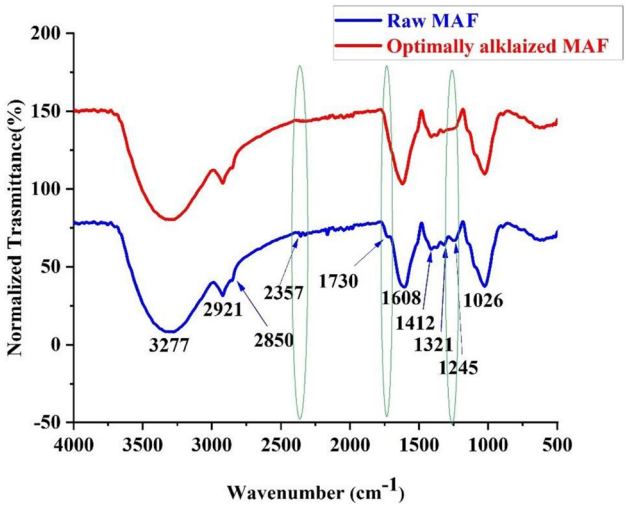

Fig. 4 FTIR spectrogram of RMAF and OAMAF

The hemicellulose fraction in the OAMAF was reduced to 7.96 ± 3.11 wt.% from 16.31 ± 3.21. The same kind of reduction in the hemicellulose content was observed in the numerous alkalized plant fibers, namely, aerial root banyan fiber (13.46 wt.% from 10.74 wt.%) and *Borassus fruit* fiber (3.02 wt.% from 14.03 wt.%) [10]. Generally, all plant fibers have a considerable amount of lignin fraction. This lignin protects the plant parts from biological attacks [45]. However, when fibers are used as reinforcement, a higher lignin fraction is believed to be a detriment as it decreased the binding capability of the cellulosic fiber with matrix materials. The lignin fraction of the OAMAF was lowered to 6.72 ± 2.88 wt.% from 14.22 ± 3.36 wt.%. Wax is another element that increased hydrophilicity [46]. After optimal alkalization, wax also reduced from 0.38 ± 0.08 wt.% to 0.18 ± 0.11 wt.%. The ash content of OAMAF increased to 9.88 ± 1.98 wt.% from 7.66 ± 2.49 wt.% as a result of an increase in the α-cellulose percentage of OAMF. The moisture in the MAF decreased to 7.04 ± 1.78 wt.% from 11.12 ± 2.11 wt.% due to the effect of alkalization [47].

3.2 Physical analysis

Usually, raw plant fibers have a lower density than alkalized plant fibers because of voids and cracks in the fibers. After alkalization, the holes and cracks in the fibers are filled by the crafted molecules, resulting in a substantial increase in fiber density. The calculated density of the OAMAF was 1136 ± 20.14 kg/m^3, which was higher than that of the RMAF [16]. Because of the removal of the outermost surface in the OAMAF, fiber diameter fell from 289 ± 21 µm to 244.3 ± 14.38 µm. The diameter of various plant fibers, namely, *Ziziphus nummularia* fiber (209.064 ± 11 to 196.24 ± 10.2 µm), *Ficus religiosa* root fiber (25.62 ± 0.951 to 22.54 ± 1.152 µm), and *Phaseolus vulgaris* fiber (352 to 345 µm), was also reduced after optimal surface modification [38]. Figure 2 shows optical microscopy pictures of RMAF and OAMAF.

3.3 Crystallographic investigation

The XRD spectra of RMAF and OAMAF are shown in Fig. 3. It highlights two rising peaks at 15° and 22° in RMAF and OAMAF, respectively. The peak with a Miller index of 1 1 0 indicated cellulose category I, whereas the peak with a Miller index of 0 0 2 indicated cellulose category IV [48]. After the alkalization, the height of both cellulose peaks was considerably enhanced because of the conversion of amorphous fraction to α-cellulose [49]. The measured CI value of the RMAF was 24.01%, whereas the CI value of the OAMAF was computed as 49.89%. It was found that the CI value of many alkalized plant fibers increased, i.e., *Ziziphus mauritiana* fiber (31.70 to 41.81%),

Table 4 Wavenumbers of noteworthy peaks in an FTIR spectrogram, linked chemical components, and associated functional groups in the RMAF and OAMAF

Stretching location (wavenumber (cm^{-1}))		Chemical components	Associated chemical functional group	Reference
Raw MAF	Optimally NaOH-treated MAF			
3277	3277	α-Cellulose	OH stretching	[51]
2921	2921	α-Cellulose	CH and CH_2 stretching	[52]
2850	2850	α-Cellulose	C–H stretching of alkanes	[53]
2357	–	Wax and other impurities	C≡C stretching	[30]
1730	–	Lignin	Carbonylic group C = O stretching	[54]
1608	1608	Hemicellulose	C = O stretching	[55]
1412	1412	Moisture particles	–	[13]
1321	1321	Cellulose	OH bending vibration	[56]
1245	–	Lignin, hemicellulose	CO stretching	[57]
1026	1026	Cellulose	C–O–C pyranose ring skeletal vibrations	[58]

Acacia planifrons bark fiber (65.38 to 74.78%), *Symphirema involucratum* fiber (28.22 to 33.33%), and *Acacia concinna* fiber (27.5 to 35.6%) [15, 23]. Another important crystallographic parameter of plant fiber is the CS, which is associated with the moisture-absorbing ability of the plant fiber [50]. Owing to crystallographic alterations, the CS value of the OAMAF reduced from 2.75 to 1.60 nm. This reduction was indicated in the previously investigated plant fibers, namely, *Coccinia grandis* L. (13.38 to 8.15 nm), *Z. mauritiana* fiber (43.5 to 33.9 nm), and *S. involucratum* fiber (5.10 to 3.21 nm) [42]. XRD, TGA, and tensile testing outcomes of RMAF, OAMAF and other cellulosic fibers are synopsized in Table 3.

3.4 Determination of chemical functional groups

Figure 4 shows the FTIR spectrograms of the RMAF and OAMAF. Ten significant peaks were observed for the RMAF, in which three peaks completely vanished after the alkalization. Table 4 contains the pertinent information on the existing peaks in the MAF. The OH stretching of α-cellulose is indicated as a first peak at 3277 cm^{-1} in the MAF spectra [51]. In both RMAF and OAMAF, the CH and CH_2 peaks of α-cellulose (2921 cm^{-1}) were also seen [52]. The C–H vibration of alkanes in α-cellulose was also revealed by a small peak at 2850 cm^{-1} [53]. After alkalization, two successive peaks at 2357 cm^{-1} (C–C stretching, wax, and other impurities) and 1730 cm^{-1} (carbonylic group C = O stretching) were eliminated of amorphous fraction in the MAF [30, 54]. C = O stretching of hemicellulose in the MAFs was revealed by the peak at 1608 cm^{-1} [55]. The peak at 1412 cm^{-1} revealed the existence of wetness in the MAF [13]. The OH bending vibration of cellulose was linked to a small peak at 1321 cm^{-1} in the RMAF and OAMAF [56]. Lignin and hemicellulose were considered absent from the optimally alkalized fiber because there was no peak at 1245 cm^{-1} [57]. It is the peak at 1026 cm^{-1} that could be used to identify the C–O–C pyranose ring vibrations (cellulose) in the fibers [58].

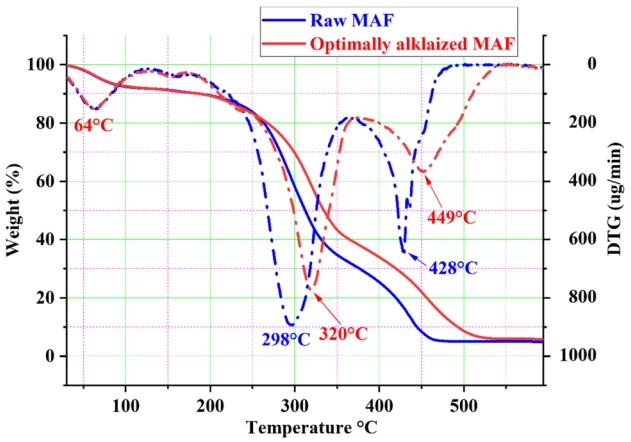

Fig. 6 TG and DTG diagrams of RMAF and OAMAF

3.5 Nuclear resonance spectroscopy

Figure 5 shows the NMR spectrums of the RMAF and OAMAF. The existence of cellulose in MAF is confirmed by 104.46 ppm of C-1 carbon. In the RMAF and OAMAF, the C-2, C-3, and C-5 are identified by the peak between 72 and 74 ppm [29]. C-1 and C-4 (cellulose) are present at 83 and 64 ppm, respectively, in both the RMAF and OAMAF [59]. In the RMAF, the carbonyl group is observed at 175 ppm, which is connected to the hemicellulose fraction of the fiber.

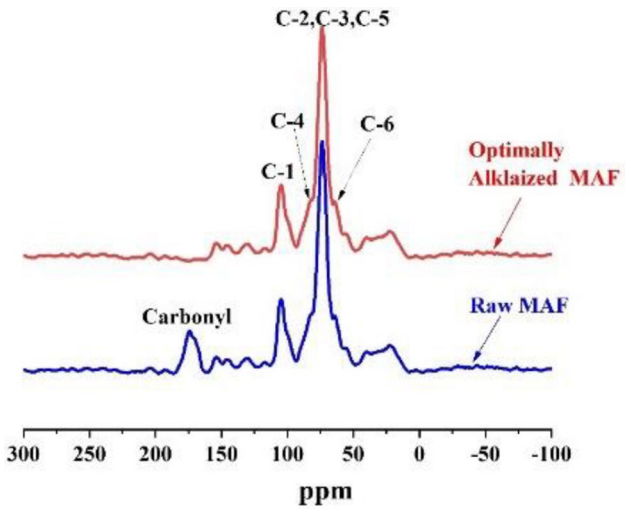

Fig. 5 NMR spectrograms of RMAF and OAMAF

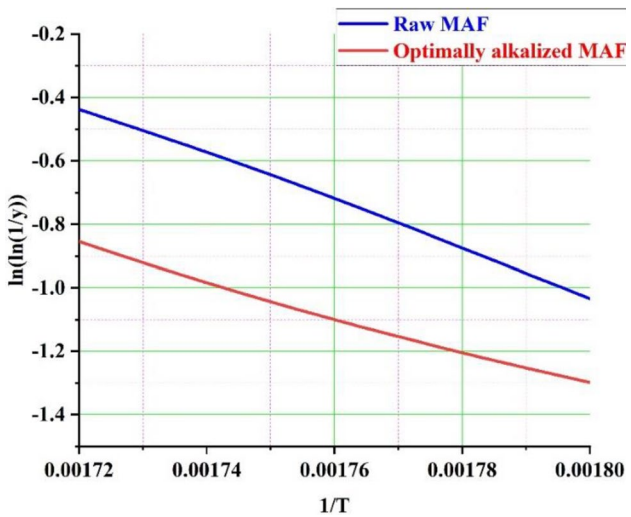

Fig. 7 Broido's profiles of the RMAF and OAMAF

In the OAMAF, the carbonyl peak disappeared, indicating the elimination of hemicellulose fraction from the OAMAF [28].

3.6 Thermogravimetric analysis

TG and DTG patterns for RMAF and OAMAF are shown in Fig. 6. It is observed that the fiber loses around 10% of its weight from 30 to 200 °C owing to disappearance of wetness [60]. In the course of the alkalization, a significant quantity of hemicellulose was transformed to α-cellulose. Because of its crystalline structure, α-cellulose is more thermally stable than hemicellulose, which is reflected in the 200 to 500 °C segment [61]. The 200 to around 350 °C portion in the TG profile connected with the thermal decomposition of hemicellulose and cellulose. The wax and lignin fraction in the MAF are degraded in the 350–500 °C range. The quantity of fiber (about 5 wt.%) retained at 594 °C, which was believed as the residual mass.

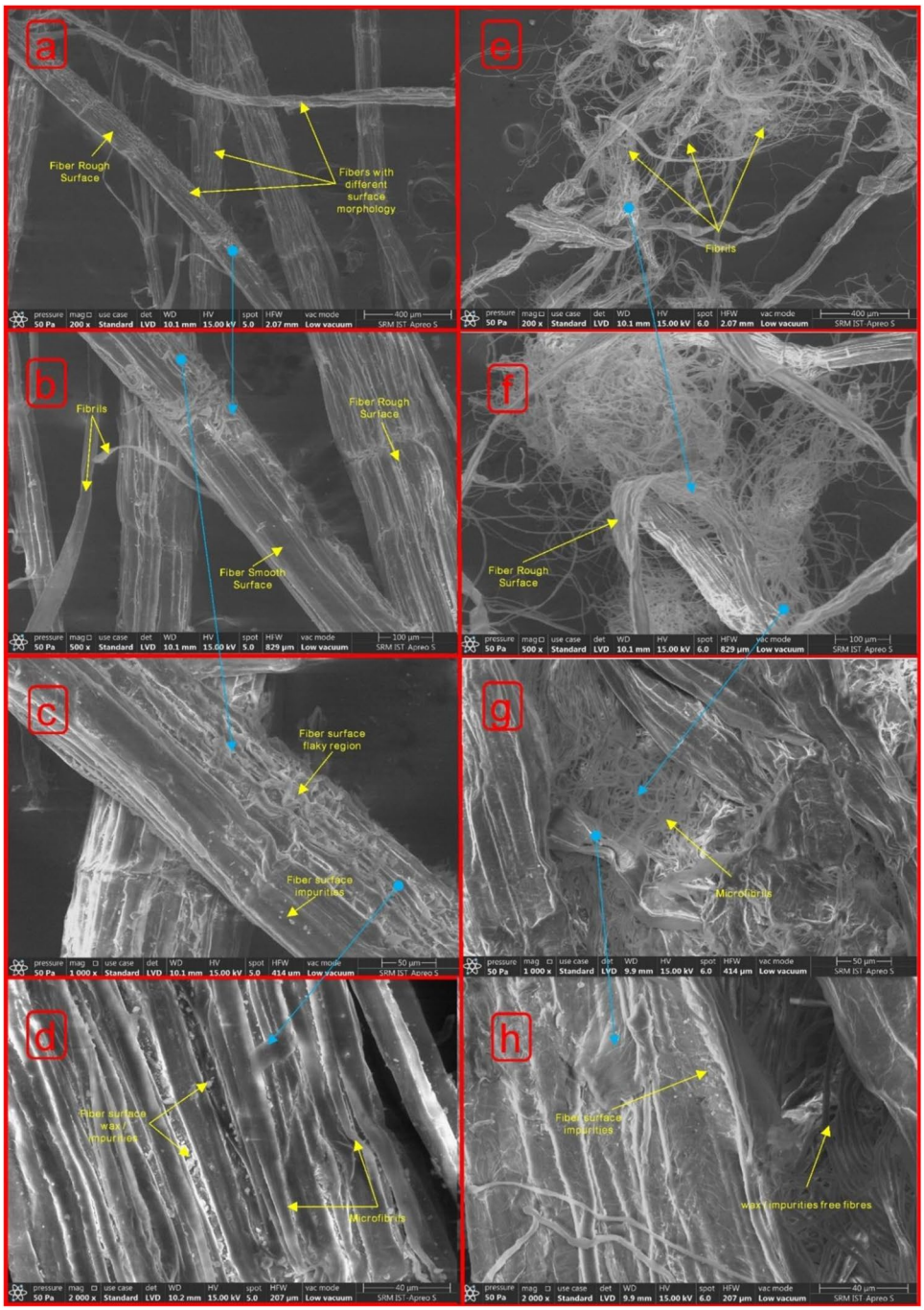

Fig. 8 SEM images of the RMAF (**a**–**d**) and OAMAF (**e**–**h**)

Three important peaks were observed in the DTG curve [62]. In both RMAF and OAMAF, the initial peak was located at 64 °C, indicating the abolition of wetness from the fiber. For RMAF, the cellulose degradation peak was found to be at 298 °C. In the OAMAF, this peak was shifted to 320 °C owing to the increase in the α-cellulose content. The same kind of improvement was reported in many plant fibers, namely, *P. vulgaris* fiber (322.1 to 346.6 °C), *Musa acuminata* peduncles fiber (337 to 350 °C), *F. religiosa* root fiber (325 to 356 °C), and *Bahunia racemosa* fiber (313–356 °C) after surface modification [21, 43]. A sharp peak witnessed around at 430 °C is linked to the degradation of the lignin in the MAFs.

Figure 7 shows Broido's profile of the RMAF and OAMAF. The E_a of the OAMAF was improved from 68.08 to 72.46 kJ/mol. RMAF and OAMAF had kinetic activation energies in the middle of the recommended range for wood (60 to 150 kJ/mol) [63]. Thermal study showed that RMAF and OAMAF could be utilized as reinforcement in polymers. However, the processing temperature of the composites should be maintained below 200 °C.

3.7 Scanning electron microscopic analysis

SEM pictures of the RMAF and OAMAF are shown in Fig. 8. Alkalization detached single fibers from the fiber bundles (Fig. 8e) whereas raw fibers were connected to the fiber bundles (Fig. 8a) [33]. Figure 8f shows that the surface roughness of OAMAF is improved, although the smoother surface of RMAF (Fig. 8b) is still present [64]. Figure 8c and d show the occurrence of wax and contaminants in the RMAF surface. Impurity-free fine fibers are seen in Fig. 8g and h [65].

3.8 Energy-dispersive X-ray analysis

EDX spectrum of the RMAF and OAMAF is revealed in Fig. 9a and b. In the EDX spectrum of the RMAF, many elements, namely, calcium (Ca), potassium (K), sulfur (S), phosphorus (P), aluminum (Al), and magnesium (Mg), are present along with carbon (C) and oxygen (O). Generally, impurity-free cellulosic fibers have only carbon (C) and oxygen (O) elements [66]. Presence of additional element indicated occurrence of contaminations on the RMAF surface. These unwanted elements vanished after the alkalization. This was indicated by the removal of a thin layer made up of contamination on the fiber [67]. In the OAMAF, a new element, sodium (Na), was observed, indicating the improper removal of sodium in the HCl treatment during the alkalization process. However, after alkalization, a small quantity of sodium content was observed in various plant fibers, namely, *A. concinna*, *Pongamia pinnata* L., *S. involucratum*, and *Cissus vitiginea* [67, 68].

3.9 Atomic force microscopic analysis

The recorded (a) three-dimensional and (b) two-dimensional images of AFM, (c) line profile of surface, and (d) morphological parameters are shown in Fig. 10. The average roughness (R_a) of the OAMAF was amplified

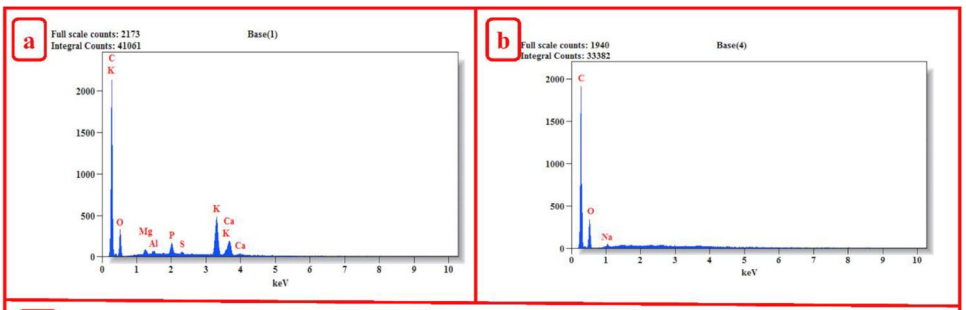

c

Element	Raw MAF		Optimally alkalized MAF	
	Weight (%)	Atomic (%)	Weight (%)	Atomic (%)
C	48.63	61.69	60.44	64.71
O	31.59	30.09	38.96	34.72
Mg	1.03	0.65	0	0
Al	0.49	0.27	0	0
P	2.00	0.98	0	0
S	0.37	0.17	0	0
K	10.81	4.21	0	0
Ca	5.08	1.93	0	0
Na	0	0	0.6	0.57

Fig. 9 EDX Spectrum of RAMF and OAMF

to 77.373 nm from 27.113 nm. Because of alkalization, improvement in the R_a value of various plant fibers such as *S. involucratum* (6.647 to 15.826 nm), *Eichhornia crassipes* (101.84 to 112.84 nm), and ariel root *Ficus amplissima* fiber (8.225 to 15.387 nm) was reported in a previous investigation [69]. This enhanced R_a value indicated the existence of an impurity-free surface [49]. The roughness skewness (R_{sk}) values of the RMAF (− 1.747) and OAMAF (− 0.141) were negative, indicating cracks and pores in the fiber [15]. However, after alkalization, pores and cracks in the fibers were significantly reduced. The R_{ku} value of the OAMAF was exceedingly reduced to below 3 (2.952 from 6.318), suggesting a high uneven surface in the fiber [70]. Other surface morphological parameters such as R_z, R_t, and R_q were enhanced considerably after optimal alkalization.

3.10 Tensile testing

Alkalization enhanced the fiber tensile strength and modulus by improved the crystalline fraction. However, improper surface modification may lead to reduced tensile strength. OAMF showed improved tensile strength of 307.3 ± 24.12 MPa whereas tensile strength of the RAMF was 274.6 ± 29.5 MPa [71]. The tensile modulus of the OAMAF also increased from 2.88 ± 1.026 GPa to

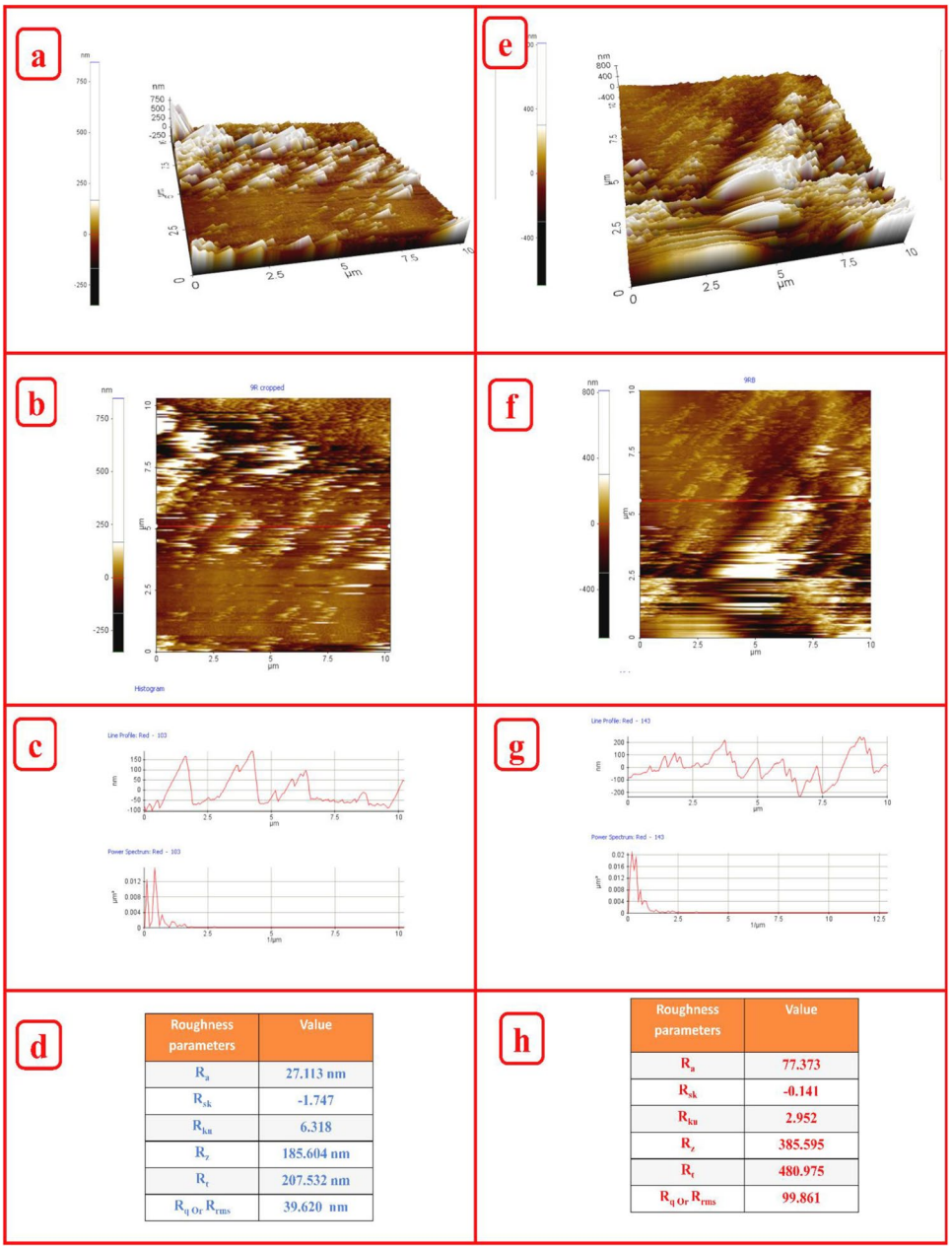

Fig. 10 **a** 3D and **b** 2D AFM images, **c** line diagram of profile, and **d** surface morphological parameters of the RMAF and OAMAF

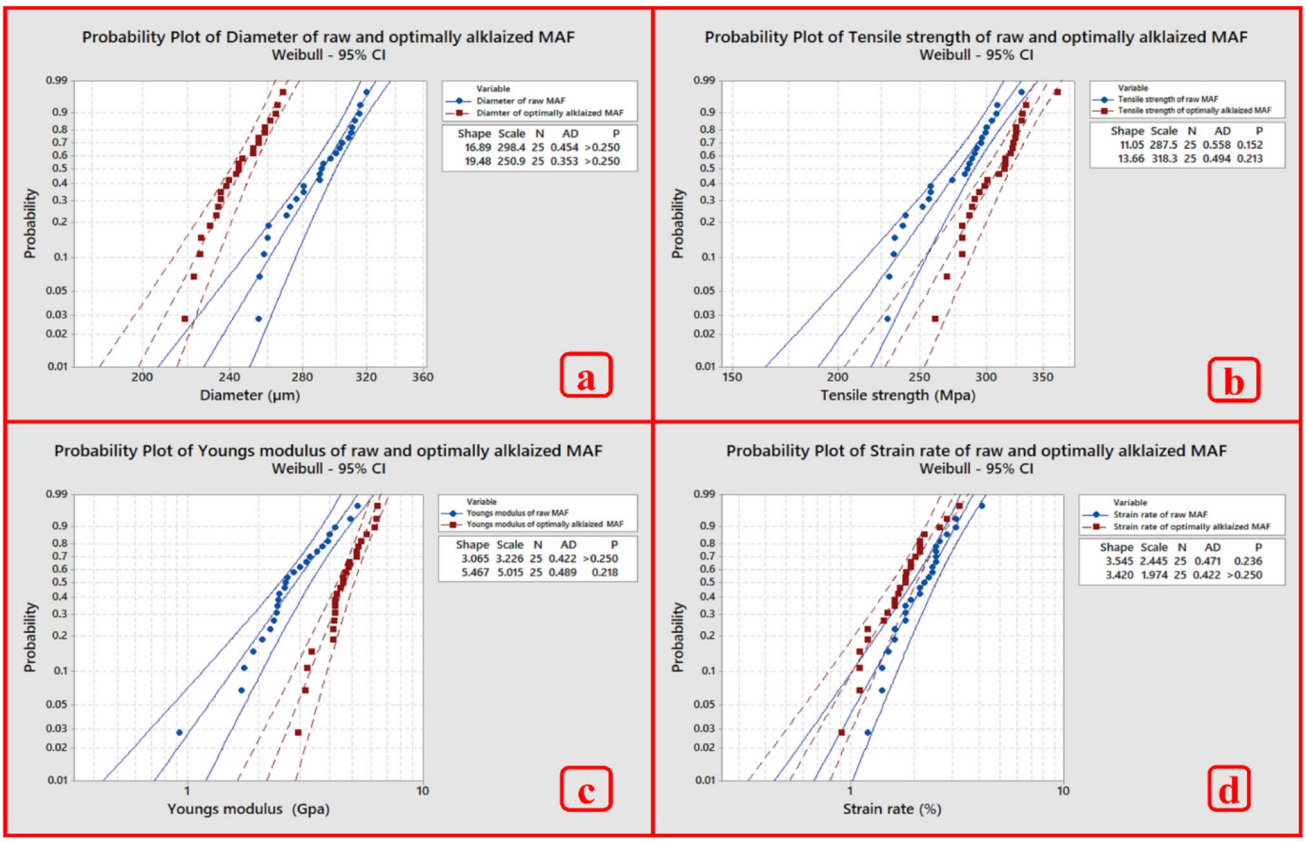

Fig. 11 Weibull analysis curves of tensile properties and diameter of the RMAF and OAMAF

4.633 ± 0.94 GPa. The strain rate of the OAMAF was decreased from 2.208 ± 0.654% to 1.776 ± 0.56%. The microfibril angle of the OAMAF was also decreased to 10.64 ± 1.65° from 11.87 ± 1.72°. The microfibril angle (α) of plant fibers improved as elongation percentages improved, and it dropped as the tensile strength and modulus increased. Owing to the variations in the shape of the fiber, maturity, and part that yields the fiber, tensile properties also differ. So, a statistical investigation method is needed to check the consistency of the mechanical property values. Figure 11 shows the Weibull distribution curves for the diameter and tensile characteristics of RMAF and OAMAF [14]. It showed that the tensile properties of the tested 25 RAMAF and OAMAFs are within the prescribed range, indicating their fitness to utilize as reinforcement in polymer matrixes.

4 Conclusions

The optimum alkalization duration for the MAF was optimized through chemical analysis. Owing to the removal of the outer most surface layer in the OAMAF, the diameter (289 ± 21 µm to 244.3 ± 14.38 µm) was reduced, whereas density (1082 ± 29 kg/m^3 to 1136 ± 20.14 kg/m^3) was slightly increased because of the filling of voids and cracks in the RMAF by grafted molecules. The CI value of the OAMAF revealed an increase in the crystalline fraction. Owing to alkalization, the hemicellulose component in the MAF was removed, as shown by the absence of peaks at 175 ppm in the NMR spectrum of OAMAF. Increases in the maximum degradation temperature and E_a of the OAMAF indicated a corresponding increase in its thermal consistency. The results of AFM showed that the R_a value amplified to 77.373 nm from 27.113 nm, designating that the surface roughness of the OAMAF increased. The results of this study indicated that OAMAF is a viable choice for consumption as reinforcement in polymers. In the future, RMAF and OAMAF-reinforced polymer composites can be developed and characterized to find suitable applications.

Author contribution P.Senthamaraikannan.: investigation, formal analysis, visualization, writing—original draft. S.S.Saravanakumar.: methodology, manuscript editing and review, supervision.

Declarations

Conflict of interest The authors declare no competing interests.

References

1. Ilangovan M, Guna V, Prajwal B et al (2020) Extraction and characterisation of natural cellulose fibers from Kigelia africana. Carbohydr Polym 236:115996. https://doi.org/10.1016/j.carbpol.2020.115996
2. Nagarajan KJ, Balaji AN, Ramanujam NR (2019) Extraction of cellulose nanofibers from cocos nucifera var aurantiaca peduncle by ball milling combined with chemical treatment. Carbohydr Polym 212:312–322. https://doi.org/10.1016/j.carbpol.2019.02.063
3. Jagadeesh P, Puttegowda M, Mavinkere Rangappa S, Siengchin S (2021) A review on extraction, chemical treatment, characterization of natural fibers and its composites for potential applications. Polym Compos 42:6239–6264. https://doi.org/10.1002/pc.26312
4. Durai PN, Viswalingam K (2022) Suitability assessment of Musa acuminata peduncles fiber for fabrication of green composites. J Nat Fibers 19:14866–14879. https://doi.org/10.1080/15440478.2022.2069191
5. Suganya G, Senthil kumar S, Jayabalakrishnan D, et al (2022) Mechanical, thermal, and fatigue behavior of aloe vera fiber/pistachio shell powder toughened epoxy resin composite. Biomass Convers Biorefinery 1:1–8. https://doi.org/10.1007/s13399-022-02787-5
6. Sreenivasan VS, Ravindran D, Manikandan V, Narayanasamy R (2011) Mechanical properties of randomly oriented short Sansevieria cylindrica fibre/polyester composites. Mater Des 32:2444–2455. https://doi.org/10.1016/j.matdes.2010.11.042
7. Selvi ST, Sunitha R, Ammayappan L, Prakash C (2022) Effect of chemical treatment on surface modification of Abutilon indicum fibres for composites applications. Biomass Convers Biorefin 1:1–9. https://doi.org/10.1007/S13399-022-03298-Z/FIGURES/6
8. Sanjay MRR, Siengchin S, Parameswaranpillai J et al (2019) A comprehensive review of techniques for natural fibers as reinforcement in composites: preparation, processing and characterization. Carbohydr Polym 207:108–121. https://doi.org/10.1016/j.carbpol.2018.11.083
9. Balaji AN, Nagarajan KJ (2017) Characterization of alkali treated and untreated new cellulosic fiber from Saharan aloe vera cactus leaves. Carbohydr Polym 174:200–208. https://doi.org/10.1016/j.carbpol.2017.06.065
10. Singh JK, Rout AK (2022) Characterization of raw and alkali-treated cellulosic fibers extracted from Borassus flabellifer L. Biomass Convers Biorefin 1:21–22. https://doi.org/10.1007/s13399-022-03238-x
11. Rathinavelu R, Sethupathi B (2022) Examination of characteristic features of raw and alkali-treated cellulosic plant fibers from Ventilago maderaspatana for composite reinforcement. Biomass Convers Biorefin https://doi.org/10.1007/s13399-022-03461-6
12. Senthamaraikannan P, Saravanakumar SSS (2022) Utilization of Mucuna atropurpurea stem fiber as a reinforcement in fiber reinforced plastics. Polym Compos 43:4959–4978. https://doi.org/10.1002/pc.26763
13. Manimaran P, Pillai GP, Vignesh V, Prithiviraj M (2020) Characterization of natural cellulosic fibers from Nendran Banana Peduncle plants. Int J Biol Macromol 162:1807–1815. https://doi.org/10.1016/j.ijbiomac.2020.08.111
14. Vijay R, Lenin Singaravelu D, Vinod A et al (2019) Characterization of raw and alkali treated new natural cellulosic fibers from Tridax procumbens. Int J Biol Macromol 125:99–108. https://doi.org/10.1016/j.ijbiomac.2018.12.056
15. Raju JSN, Depoures MV, Kumaran P (2021) Comprehensive characterization of raw and alkali (NaOH) treated natural fibers from Symphirema involucratum stem. Int J Biol Macromol 186:886–896. https://doi.org/10.1016/j.ijbiomac.2021.07.061
16. Narayanasamy P, Balasundar P, Senthil S et al (2020) Characterization of a novel natural cellulosic fiber from Calotropis gigantea fruit bunch for ecofriendly polymer composites. Int J Biol Macromol 150:793–801. https://doi.org/10.1016/j.ijbiomac.2020.02.134
17. Kurschner K, Hoffer A (1933) Cellulose and cellulose derivative. Fresenius' J Anal Chem 92:145–154
18. Jaiswal D, Devnani GLL, Rajeshkumar G et al (2022) Review on extraction, characterization, surface treatment and thermal degradation analysis of new cellulosic fibers as sustainable reinforcement in polymer composites. Curr Res Green Sustain Chem 5:100271. https://doi.org/10.1016/j.crgsc.2022.100271
19. APPITA Testing Committee A (1978) Klason lignin in wood and pulp
20. Conrad CM (1944) Determination of wax in cotton fiber a new alcohol extraction method. Ind Eng Chem - Anal Ed 16:745–748. https://doi.org/10.1021/i560136a007
21. Moshi AM, D. R, S.R. SB, et al (2020) Characterization of surface-modified natural cellulosic fiber extracted from the root of Ficus religiosa tree. Int J Biol Macromol 156:997–1006. https://doi.org/10.1016/j.ijbiomac.2020.04.117
22. Tiwari YM, Sarangi SK (2022) Characterization of raw and alkali treated cellulosic Grewia flavescens natural fiber. Int J Biol Macromol 209:1933–1942. https://doi.org/10.1016/j.ijbiomac.2022.04.169
23. Venugopal A, Boominathan SK (2020) Physico-chemical, thermal and tensile properties of alkali-treated Acacia concinna fiber. J Nat Fibers 00:1–16. https://doi.org/10.1080/15440478.2020.1838998
24. Manimaran P, Saravanan SPP, Sanjay MRR et al (2020) New lignocellulosic Aristida adscensionis fibers as novel reinforcement for composite materials: extraction, characterization and Weibull distribution analysis. J Polym Environ 28:803–811. https://doi.org/10.1007/s10924-019-01640-7
25. Rajeshkumar G, Hariharan V, Scalici T (2016) Effect of NaOH treatment on properties of Phoenix Sp. fiber. J Nat Fibers 13:702–713. https://doi.org/10.1080/15440478.2015.1130005
26. Segal L, Creely JJ, Martin AE, Conrad CM (1959) An empirical method for estimating the degree of crystallinity of native cellulose using the X-ray diffractometer. Text Res J 29:786–794. https://doi.org/10.1177/004051755902901003
27. Keskin OY, Koktas S, Seki Y et al (2022) Natural cellulosic fiber from Carex panicea stem for polymer composites: extraction and characterization. Biomass Convers Biorefinery 18:644–652. https://doi.org/10.1007/s13399-022-03458-1
28. Palai BKBK, Sarangi SKSK (2022) Characterization of untreated and alkalized Eichhornia crassipes fibers and its composites. J Nat Fibers 19:3809–3824. https://doi.org/10.1080/15440478.2020.1848729
29. Sudhir Chakravarthy K, Madhu S, Raju JSN, Jabihulla Shariff MD (2020) Characterization of novel natural cellulosic fiber extracted from the stem of Cissus vitiginea plant. Int J Biol Macromol 161:1358–1370. https://doi.org/10.1016/j.ijbiomac.2020.07.230
30. Cheng D, Weng B, Chen Y et al (2020) Characterization of potential cellulose fiber from Luffa vine: a study on physicochemical and structural properties. Int J Biol Macromol 164:2247–2257. https://doi.org/10.1016/j.ijbiomac.2020.08.098
31. Liu Y, Xie J, Wu N et al (2019) Characterization of natural cellulose fiber from corn stalk waste subjected to different surface treatments. Cellulose 26:4707–4719. https://doi.org/10.1007/s10570-019-02429-6
32. Broido A (1969) A simple, sensitive graphical method of treating thermogravimetric analysis data. J Polym Sci Part A-2 Polym Phys 7:1761–1773. https://doi.org/10.1002/pol.1969.160071012
33. Fiore V, Scalici T, Valenza A (2014) Characterization of a new natural fiber from Arundo donax L. as potential reinforcement of polymer composites. Carbohydr Polym 106:77–83. https://doi.org/10.1016/j.carbpol.2014.02.016
34. Indran S, Edwin Raj R, Sreenivasan VS (2014) Characterization of new natural cellulosic fiber from Cissus quadrangularis root.

Carbohydr Polym 110:423–429. https://doi.org/10.1016/j.carbpol.2014.04.051
35. Sabarinathan P, Rajkumar K, Annamalai VE, Vishal K (2020) Characterization on chemical and mechanical properties of silane treated fish tail palm fibres. Int J Biol Macromol 163:2457–2464. https://doi.org/10.1016/j.ijbiomac.2020.09.159
36. Indran S, Raj REE (2015) Characterization of new natural cellulosic fiber from Cissus quadrangularis stem. Carbohydr Polym 117:392–399. https://doi.org/10.1016/j.carbpol.2014.09.072
37. Perumal L, Sarala, (2020) Characterization of a new natural cellulosic fiber extracted from Derris scandens stem. Int J Biol Macromol 165:2303–2313. https://doi.org/10.1016/j.ijbiomac.2020.10.086
38. Gurupranes IR, N SS, (2022) Suitability assessment of raw-alkalized Ziziphus nummularia bark fibers and its polymeric composites for lightweight applications. Polym Compos 43:5059–5075. https://doi.org/10.1002/pc.26782
39. Mansingh B, Joseph Selvi B, Abu Hassan S et al (2021) Characterization of chemically treated new natural cellulosic fibers from peduncle of Cocos nucifera L Var typica. Polym Compos 42:6403–6416. https://doi.org/10.1002/pc.26307
40. Boopathi L, Sampath PS, Mylsamy K (2012) Investigation of physical, chemical and mechanical properties of raw and alkali treated Borassus fruit fiber. Compos Part B Eng 43:3044–3052. https://doi.org/10.1016/j.compositesb.2012.05.002
41. Durai PN, Viswalingam K, Devi MR (2022) Mechanical, surface morphological, and thermal properties of Musa acuminate peduncles fiber reinforced polyester composites: Fiber loading and alkalization impact. Polym Compos 43:4919–4929. https://doi.org/10.1002/pc.26752
42. Vinod A, Vijay R, Lenin Singaravelu D et al (2020) Effect of alkali treatment on performance characterization of Ziziphus mauritiana fiber and its epoxy composites. J Ind Text 51:2444S-2466S. https://doi.org/10.1177/1528083720942614
43. Aseer JR, K S, Bahubalendruni MVAR, et al (2022) Cellulosic microfiber extraction from ecofriendly Bahunia racemosa and its characterization. J Nat Fibers 19:14477–14489. https://doi.org/10.1080/15440478.2022.2064400
44. Rameshkannan G, Ramesh Babu S (2022) Effect of alkalization on physical, chemical, morphological and mechanical properties of arial root Ficus amplissima fibre. J Nat Fibers 19:12129–12143. https://doi.org/10.1080/15440478.2022.2051671
45. Rathinavelu R, Arumugam E, Paramathma BS (2022) Suitability examination of a new cellulosic fiber extracted from the stem of Ventilago maderaspatana plant as polymer composite reinforcement. Polym Compos 43:3015–3028. https://doi.org/10.1002/pc.26596
46. Rathinavelu R, Paramathma BS (2022) Comprehensive characterization of Echinochloa frumentacea leaf fiber as a novel reinforcement for composite applications. Polym Compos 43:5031–5046. https://doi.org/10.1002/pc.26775
47. Ramesh G, Subramanian K, Sathiyamurthy S, Jayabal S (2020) Study on influence of fiber length and fiber weight proportion in mechanical behavior of Calotropis gigantea fiber-epoxy composites. Polym Compos 41:4899–4906. https://doi.org/10.1002/pc.25761
48. Belouadah Z, Toubal LM, Belhaneche-Bensemra N, Ati A (2020) Characterization of ligno-cellulosic fiber extracted from Atriplex halimus L. plant. Int J Biol Macromol 168:806–815. https://doi.org/10.1016/j.ijbiomac.2020.11.142
49. Shanmugasundaram N, Rajendran I, Ramkumar T (2018) Characterization of untreated and alkali treated new cellulosic fiber from an Areca palm leaf stalk as potential reinforcement in polymer composites. Carbohydr Polym 195:566–575. https://doi.org/10.1016/j.carbpol.2018.04.127
50. Liu Y, Lv X, Bao J et al (2019) Characterization of silane treated and untreated natural cellulosic fibre from corn stalk waste as potential reinforcement in polymer composites. Carbohydr Polym. https://doi.org/10.1016/j.carbpol.2019.04.088
51. Gupta US, Tiwari S (2022) Mechanical and surface characterization of sisal fibers after cold glow discharge argon plasma treatment. Biomass Convers Biorefin 1:1–15. https://doi.org/10.1007/S13399-022-03247-W/FIGURES/10
52. Maache M, Bezazi A, Amroune S et al (2017) Characterization of a novel natural cellulosic fiber from Juncus effusus L. Carbohydr Polym 171:163–172. https://doi.org/10.1016/j.carbpol.2017.04.096
53. Ray R, Mohapatra A, Das SN et al (2020) Comprehensive characterization of a novel natural Bauhinia vahlii stem fiber. Polym Compos 41:1–10. https://doi.org/10.1002/pc.25678
54. Vinod MRS, Siengchin S (2021) Fatigue and thermo-mechanical properties of chemically treated Morinda citrifolia fiber-reinforced bio-epoxy composite: a sustainable green material for cleaner production. J Clean Prod 326:129411. https://doi.org/10.1016/j.jclepro.2021.129411
55. Rajeshkumar G, Arvindh Seshadri S, Devnani GLL et al (2021) Environment friendly, renewable and sustainable poly lactic acid (PLA) based natural fiber reinforced composites – A comprehensive review. Elsevier Ltd
56. Binoj JSS, Edwin Raj R, Daniel BSSSS (2017) Comprehensive characterization of industrially discarded fruit fiber, Tamarindus indica L. as a potential eco-friendly bio-reinforcement for polymer composite. J Clean Prod 142:1321–1331. https://doi.org/10.1016/j.jclepro.2016.09.179
57. Sonia A, Priya Dasan K (2013) Chemical, morphology and thermal evaluation of cellulose microfibers obtained from Hibiscus sabdariffa. Carbohydr Polym 92:668–674. https://doi.org/10.1016/j.carbpol.2012.09.015
58. Subramanya R, Satyanarayana KG, Shetty Pilar B (2017) Evaluation of structural, tensile and thermal properties of banana fibers. J Nat Fibers 14:485–497. https://doi.org/10.1080/15440478.2016.1212771
59. jabihulla Shariff M, Madhu S, Chakravarthy KS, Siva Naga Raju J (2022) Characterization of natural cellulose fibers from the stem of Albizia julibrissin as reinforcement for polymer composites. J Nat Fibers 19:2204–2217. https://doi.org/10.1080/15440478.2020.1807440
60. Gond RK, Gupta MK (2020) A novel approach for isolation of nanofibers from sugarcane bagasse and its characterization for packaging applications. Polym Compos 41:5216–5226. https://doi.org/10.1002/pc.25788
61. S. S, K. M, (2022) Use of Pennisetum glaucum stem powder waste as reinforcement in epoxy composites. Polym Compos 43:4998–5010. https://doi.org/10.1002/pc.26773
62. Somasundaram R, Rajamoni R, Suyambulingam I et al (2022) Utilization of discarded Cymbopogon flexuosus root waste as a novel lignocellulosic fiber for lightweight polymer composite application. Polym Compos 43:2838–2853. https://doi.org/10.1002/pc.26580
63. Belouadah Z, Ati A, Rokbi M (2015) Characterization of new natural cellulosic fiber from Lygeum spartum L. Carbohydr Polym 134:429–437. https://doi.org/10.1016/j.carbpol.2015.08.024
64. Gillela S, Yadav SM, Sihag K et al (2022) A review on Lantana camara lignocellulose fiber-reinforced polymer composites. Biomass Convers Biorefin 1:1–19
65. Bharath KNN, Madhu P, Gowda TGYGYY et al (2020) Alkaline effect on characterization of discarded waste of Moringa oleifera fiber as a potential eco-friendly reinforcement for biocomposites. J Polym Environ 28:2823–2836. https://doi.org/10.1007/s10924-020-01818-4

66. Rashid B, Leman Z, Jawaid M et al (2016) Physicochemical and thermal properties of lignocellulosic fiber from sugar palm fibers: effect of treatment. Cellulose 23:2905–2916. https://doi.org/10.1007/s10570-016-1005-z
67. Umashankaran M, Gopalakrishnan S (2021) Effect of sodium hydroxide treatment on physico-chemical, thermal, tensile and surface morphological properties of Pongamia pinnata L. bark fiber. J Nat Fibers 18:2063–2076. https://doi.org/10.1080/15440478.2019.1711287
68. Katragadda SC, Sundaram M, Palani K (2022) Characterization of optimally alkali-treated natural cellulosic fiber extracted from the stem of Cissus vitiginea plant. J Nat Fibers 19:9139–9152. https://doi.org/10.1080/15440478.2021.1982443
69. Palai BKBK, Sarangi SKSK (2021) Suitability evaluation of untreated and surface-modified Eichhornia crassipes fibers for brake pad applications. J Nat Fibers 00:1–14. https://doi.org/10.1080/15440478.2021.1875379
70. Prithiviraj M, Muralikannan R (2022) Investigation of optimal alkali-treated Perotis indica plant fibers on physical, chemical, and morphological properties. J Nat Fibers 19:2730–2743. https://doi.org/10.1080/15440478.2020.1821291
71. Rajeshkumar G, Hariharan V, Indran S et al (2020) Influence of sodium hydroxide (NaOH) treatment on mechanical properties and morphological behaviour of Phoenix sp Fiber/Epoxy Composites. J Polym Environ 29:765–774. https://doi.org/10.1007/s10924-020-01921-6